

Fate of separate chiral transitions at finite μ_I under the influence of mismatched vector interactions

Zhao Zhang* and Hai-Peng Su

School of Mathematics and Physics, North China Electric Power University, Beijing 102206, China

(Dated: February 27, 2022)

The flavor-mixing induced by the mismatched vector-isoscalar and vector-isovector interactions at finite baryon chemical potential μ and isospin chemical potential μ_I is demonstrated in the Nambu-Jona-Lasinio (NJL) type model of QCD. The influence of this non-anomaly flavor-mixing on the possible separate chiral transitions at nonzero μ_I is studied under the assumption of the effective restoration of the $U(1)_A$ symmetry. We find that for the weak isospin asymmetry, the two separate phase boundaries found previously can be converted into one only if the vector-isovector coupling g_v^v is significantly stronger than the vector-isoscalar one g_v^s without the axial anomaly. When the weak Kabayashi-Maskawa-'t Hooft (KMT) interaction is included, we find that the separation of the chiral transition with two critical endpoints for the relatively strong isospin asymmetry can still be removed owing to the vector interactions. In this case, it is not the vector coupling difference but the strength of g_v^v which is crucial for the only phase boundary. We also point out that, in the NJL-type model with mismatched vector interactions, the recently proposed equivalence for chiral transitions at finite μ and μ_I does not hold even at the mean field approximation.

PACS number(s): 12.38.Aw; 11.30.RD; 12.38.Lg;

I. INTRODUCTION

The QCD phase diagram at finite temperature T and quark chemical potential μ has attracted growing interests. Especially, a chiral critical endpoint is predicted by some models which separates the first-order transition and the smooth crossover. Such a point may locate at relatively higher T and lower μ and hence is promising to be explored in heavy ion collisions. Experimentally, the search for the critical endpoint is ongoing at RHIC (BES) [1] and will be performed in the future facilities in GSI (FAIR) and JINR (NICA). Theoretically, the existence and location of the critical endpoint are still under debate because of the limitation of the lattice QCD computations at finite μ [2] and the lack of other reliable theoretical methods for the non-perturbative dense QCD. Moreover, unconventional multiple critical endpoints for the chiral transition are also proposed by some authors using effective theories of QCD: It is found in [3, 4] that the finite isospin chemical potential μ_I may lead to the separate chiral transitions with two critical endpoints; when considering the color superconductivity (CSC), the low-temperature chiral critical endpoint(s) may appear due to the interplay between the chiral and diquark condensates [5–9].

It is generally expected that the $U(1)_A$ anomaly may impact the QCD phase transition significantly [10]. This point has been confirmed in model studies or Ginzberg-Landau analyses, where the $U(1)_A$ anomaly is usually incorporated by introducing the Kabayashi-Maskawa-'t Hooft (KMT) interaction [11, 12]. The KMT interaction explicitly breaks the $U(1)_A$ symmetry and gives rise

to the flavor-mixing among light quarks: In the chiral symmetry breaking phase, the u quark mass may contain contributions from both d and s quark condensates; for moderate or high baryon density, the diquark condensate for u-d pairing may make contribution to the s quark mass. As consequence, the $U(1)_A$ anomaly may affect not only the properties of the traditional critical endpoint [13], but also the fate of the unconventional one: the two critical endpoints due to nonzero μ_I [3, 4] may be removed by the anomaly flavor-mixing [14]; a new low-temperature critical endpoint could be induced in the presence of the color flavor locking (CFL) CSC [6].

Even the $U(1)_A$ anomaly may influence the QCD phase transition in a nontrivial way, its effect could be suppressed significantly near the phase boundary. The recent lattice calculations indicate that the $U(1)_A$ symmetry may be restored obviously near and above T_c for zero μ [15, 16]. The effective restoration of the $U(1)_A$ symmetry would influence the universality class and critical properties of the chiral transition [17]. Namely, the standard analysis assuming the symmetry restoration pattern from $SU(2)_L \otimes SU(2)_R \otimes U(1)_V$ to $SU(2)_V \otimes U(1)_V$ [10] can not be applied directly. Phenomenologically, the chiral model study suggests that the location and even the existence of the conventional critical endpoint are quite sensitive to the degree of the $U(1)_A$ symmetry restoration [13]. If the anomaly related flavor-mixing is very weak near the phase boundary, the low-temperature critical endpoint due to the CFL phase [6] may be directly ruled out; in contrast, the two critical endpoints due to the isospin asymmetry [3, 4] could be still possible because of the decouple of light quarks.

Nevertheless, it is also probable that the non-anomaly flavor-mixing of light quarks can be induced by other ingredients of QCD, especially under some condition. The main purpose of this paper is to study the possible non-

*Electronic address: zhaozhang@pku.org.cn

anomaly flavor-mixing and its effect on the chiral phase transition at finite temperature and density under the isospin asymmetry. In particular, we will concentrate on the fate of the two critical endpoints due to the separate chiral transitions found in [3, 4] with the assumption of the effective restoration of the $U(1)_A$ symmetry near the phase boundary. In addition, the validity of the recently proposed phase quenching in the mean field approximation (MFA) of QCD-models at finite μ and μ_I [18, 19] will be checked by taking into account the non-anomaly flavor-mixing.

Our starting point is the four-quark vector interactions with different coupling strengths in the isovector and isoscalar channels. In the literature, the role of vector interactions on the chiral transition has been extensively studied in the NJL-type model of QCD. A well-known result is that the chiral transition at finite μ is weakened by the vector-isoscalar interaction $g_v^s(\bar{\psi}\gamma_\mu\psi)^2$ and it would be no critical point for strong g_v^s [5, 8, 13, 20, 21]. When considering the two-flavor CSC, it is found that the g_v^s in a proper range can lead to the new low-temperature critical endpoint(s) [5], especially under the constraint of electric-charge neutrality [8, 9]¹. The sufficiently strong g_v^s is also used to account for the shrinkage of the first-order region in the quark mass plane [21]. On the other hand, the chromomagnetic instability for the two-flavor neutral CSC is found to be suppressed by the vector-isovector interaction $g_v^v(\bar{\psi}\vec{\tau}\gamma_\mu\psi)^2$ [8]. It is also demonstrated in [22–24] that both vector interactions play important role in reproducing the lattice flavor diagonal and off-diagonal susceptibilities at finite T and μ . In general, the g_v^v and g_v^s are independent coupling constants under the condition of chiral symmetry. As far as we know, the non-anomaly flavor-mixing due to the mismatched vector interactions in the vacuum has been discussed in Ref. [25] based on a three-flavor NJL model. However, the effect of the possible non-anomaly flavor-mixing at finite temperature and density is ignored in all the previous studies, which will be investigated in this paper.

The main part of this work can be regarded as an extension of Ref. [14] by including the vector interactions, where the roles of the non-anomaly flavor-mixing and the vector-isovector interaction are focused on with the assumption of the effective suppression of the $U(1)_A$ anomaly. The paper is organized as follows. In Sec.II, the extended NJL model with the vector interactions is introduced and the arguments for the vector coupling difference are given. In Sec.III, we show that the non-anomaly flavor-mixing arises at nonzero μ and μ_I due to the mismatched vector interactions. The effects of the vector interactions on the separation of the chiral transition and the validity of the phase quenching at finite μ

and μ_I are demonstrated in Sec.IV. In Sec.V, we discuss and summarize.

II. EXTENDED NJL-TYPE MODEL WITH MISMATCHED VECTOR INTERACTIONS

A. The general four-quark interaction model with mismatched vector interactions under the chiral symmetry

We start with the following Lagrangian of four-quark interaction model for two-flavor QCD

$$\mathcal{L}^{(4)} = \mathcal{L}_{\text{sym}}^{(4)} + \mathcal{L}_{\text{det}}^{(4)}, \quad (1)$$

with

$$\begin{aligned} \mathcal{L}_{\text{sym}}^{(4)} = & g_{s1} \sum_{a=0}^3 [(\bar{\psi}\tau^a\psi)^2 + (\bar{\psi}\tau^a i\gamma_5\psi)^2] \\ & - g_{v2} \sum_{a=0}^3 [(\bar{\psi}\tau^a\gamma_\mu\psi)^2 + (\bar{\psi}\tau^a\gamma_\mu\gamma_5\psi)^2] \\ & - g_{v3} [(\bar{\psi}\tau^0\gamma_\mu\psi)^2 + (\bar{\psi}\tau^0\gamma_\mu\gamma_5\psi)^2] \\ & - g_{v4} [(\bar{\psi}\tau^0\gamma_\mu\psi)^2 - (\bar{\psi}\tau^0\gamma_\mu\gamma_5\psi)^2] \end{aligned} \quad (2)$$

and

$$\begin{aligned} \mathcal{L}_{\text{det}}^{(4)} = & g_{s2} \{ \det[\bar{\psi}(1 - \gamma_5)\psi] + h.c. \} \\ = & g_{s2} [(\bar{\psi}\psi)^2 - (\bar{\psi}\vec{\tau}\psi)^2 - (\bar{\psi}i\gamma_5\psi)^2 + (\bar{\psi}\vec{\tau}i\gamma_5\psi)^2], \end{aligned} \quad (3)$$

where τ^0 , and $\vec{\tau}$ refer to the unit matrix and Pauli matrices in the flavor space, respectively. The former term $\mathcal{L}_{\text{sym}}^{(4)}$ in (1) is the general Fierz-invariant form of the four-quark interactions in color-singlet channels which respecting the global flavor symmetries of $SU(2)_V \otimes SU(2)_A \otimes U(1)_V \otimes U(1)_A$ [26]. The latter one $\mathcal{L}_{\text{det}}^{(4)}$ is the KMT interaction induced by the gauge configurations of instanton and anti-instanton [11], which only possesses the $SU(2)_V \otimes SU(2)_A \otimes U(1)_V$ global flavor symmetries.

As mentioned, we will focus on the flavor-mixing arising from the mismatched vector interactions at finite density. We see that three of the four independent coupling constants in $\mathcal{L}_{\text{sym}}^{(4)}$ are related to the vector and axial vector interactions. Generally, the nonzero sum $g_{v3} + g_{v4}$ implies that the vector coupling strength in the isovector channel is different from that in the isoscalar one. Namely, these two coupling constants are independent of each other under the chiral symmetry. Similarly, the non-vanishing $g_{v3} - g_{v4}$ indicates the mismatched axial-vector interactions in the isovector and isoscalar channels. How the vector coupling difference gives rise to the non-anomaly flavor-mixing at finite density will be detailed in next section.

Since we mainly study the chiral phase transition in the MFA, the axial-vector interactions in Lagrangian (1)

¹ Note that under the electric-charge neutrality, the electric chemical potential influences the chiral phase transition in the similar way as the isoscalar vector interaction [7].

will be ignored². Hence in our calculations, we only consider the the following effective Lagrangian

$$\begin{aligned}\mathcal{L}_{\text{eff}}^{(4)} = & g_{s1} \sum_{a=0}^3 [(\bar{\psi}\tau^a\psi)^2 + (\bar{\psi}\tau^a i\gamma_5\psi)^2] \\ & + g_{s2} [(\bar{\psi}\psi)^2 - (\bar{\psi}\vec{\tau}\psi)^2 - (\bar{\psi}i\gamma_5\psi)^2 + (\bar{\psi}\vec{\tau}i\gamma_5\psi)^2] \\ & - g_v^s (\bar{\psi}\gamma_\mu\psi)^2 - g_v^v (\bar{\psi}\vec{\tau}\gamma_\mu\psi)^2,\end{aligned}\quad (4)$$

where the independent coupling constants are reduced to four.

B. Unequal vector coupling constants in the mean field Hartree-Fock approximation

Here we stress that the vector coupling difference in the MFA can also arise from a very popular version of the NJL model [26]

$$\begin{aligned}\mathcal{L}^{(4)} = & g_{s1} \sum_{a=0}^3 [(\bar{\psi}\tau^a\psi)^2 + (\bar{\psi}\tau^a i\gamma_5\psi)^2] \\ & + g_{s2} [(\bar{\psi}\psi)^2 - (\bar{\psi}\vec{\tau}\psi)^2 - (\bar{\psi}i\gamma_5\psi)^2 + (\bar{\psi}\vec{\tau}i\gamma_5\psi)^2] \\ & - g_v \sum_{a=0}^3 [(\bar{\psi}\tau^a\gamma_\mu\psi)^2 + (\bar{\psi}\tau^a\gamma_\mu\gamma_5\psi)^2],\end{aligned}\quad (5)$$

in which only one vector coupling g_v is adopted. In the Hartree approximation, there is no difference between the coupling strengths of the two vector interactions at the mean field level for Lagrangian (5).

However, the effective vector couplings (in the sense of direct interaction) in the isoscalar and isovector channels will differ from each other if the Fock contribution is also considered. For a four-fermion interaction, the Fock contribution can be easily evaluated according to its Fierz transformation [26]. Taking into account the exchange terms, the effective direct four-quark interactions of the Lagrangian (5) take the following form:

$$\begin{aligned}\mathcal{L}_{\text{eff-direct}}^{(4)} = & \mathcal{L}^{(4)} + \mathcal{L}_{\text{Fock}}^{(4)} \\ = & (g_{s1} + g_{s2} + \frac{g_{s2}}{2N_c})[(\bar{\psi}\psi)^2 + (\bar{\psi}i\gamma_5\vec{\tau}\psi)^2] \\ & + (g_{s1} - g_{s2} - \frac{g_{s2}}{2N_c})[(\bar{\psi}\vec{\tau}\psi)^2 + (\bar{\psi}i\gamma_5\psi)^2] \\ & - g_v \sum_{a=0}^3 [(\bar{\psi}\tau^a\gamma_\mu\psi)^2 + (\bar{\psi}\tau^a\gamma_\mu\gamma_5\psi)^2] \\ & - (\frac{g_v}{N_c} + \frac{1}{2}\frac{g_{s1}}{N_c})(\bar{\psi}\tau^0\gamma_\mu\psi)^2 \\ & - (\frac{g_v}{N_c} - \frac{1}{2}\frac{g_{s1}}{N_c})(\bar{\psi}\tau^0\gamma_\mu\gamma_5\psi)^2,\end{aligned}\quad (6)$$

where N_c is the color number of the quarks. The effective Lagrangian (6) clearly shows that the exchange terms give rise to the vector coupling difference in the Hartree-Fock approximation (HFA), which is at the order of $O(1/N_c)$ compared to g_{s1} and g_v . Note that the similar result in a three-flavor NJL model has been given in [25], where the influence of the induced non-anomaly flavor-mixing on the spin content of the nucleon is investigated.

If both g_v and g_{s1} in (5) originate from the color current-current interaction $g(\bar{\psi}\gamma_\mu\lambda_c^a\psi)^2$, they fulfill the relation $g_v = g_{s1}/2$ according to the Fierz transformation. In this case, the vector coupling difference shown in (6) becomes

$$\delta g_v = g_v^s - g_v^v = \frac{2}{N_c}g_v = \frac{g_{s1}}{N_c}. \quad (7)$$

This equation indicates that the g_v^s in (4) may be larger than the g_v^v and their difference is considerable compared to g_v or g_{s1} for $N_c = 3$. However, there is no coupling strength difference between the isoscalar and isovector axial-vector interactions in the HFA for this situation.

C. Constraints on the vector interactions from the lattice chiral curvatures

Even Eq. (7) implies that the coupling g_v^v is weaker than the g_v^s , it is also possible that the g_v^v may be stronger than the g_v^s . This can be understood from the curvature difference for the chiral phase transition at finite baryon and isospin chemical potentials obtained in recent lattice calculations [28].

For small baryon and/or isospin densities, the chemical potential dependence of the pseudo-critical temperature for the chiral crossover can be expressed as

$$T_c(\mu_q, \mu_i) = T_c + A_q\mu_q^2 + B_i\mu_i^2 + O(\mu_{q/i}^4, \mu_q^2\mu_i^2), \quad (8)$$

where T_c is the chiral pseudo-critical temperature at zero quark chemical potential (In this subsection, μ_q and μ_i are used to refer to the quark baryon and isospin chemical potentials, respectively). Notice that $T_c(\mu_q, \mu_i)$ is an even function of $\mu_{q/i}$ [29]. So at the order of $\mu_{q/i}^2$, we can expand $T_c(\mu_{q/i}^2)$ as

$$T_c(\mu_{q/i}^2) = T_c(1 - \kappa_{q/i}\frac{\mu_{q/i}^2}{T_c^2}), \quad (9)$$

where the two chiral curvatures are defined as

$$\kappa_{q/i} = -T_c \frac{dT_c(\mu^2)}{d\mu_{q/i}^2}|_{\mu=0}. \quad (10)$$

The lattice QCD simulation in [28] suggests that the curvature κ_q is about 10% greater than κ_i .

Recently, the role of the vector coupling strength g_v^s on the determination of κ_q has been studied in a Polyakov-loop enhanced three-flavor NJL model [13]. It is found

² The axial-vector interaction may be responsible for the deviation of the chiral magnetic effect in the recent lattice calculation compared to the analytic formula, as proposed in Ref. [27].

that the κ_q decreases with the g_v^s and to reproduce the lattice κ_q in this model the g_v^s must keep relatively larger value compared to the scalar coupling strength g_s . The authors of Ref. [13] then propose the lattice κ_q can be used as a useful constraint on the strength of g_v^s .

We can directly extend this idea to determine the κ_i by replacing μ_q with μ_i . As will be demonstrated in the next section, the coupling g_v^v influences the curvature κ_i in the similar way as the g_v^s does on the κ_q . In particular, the κ_i and κ_q obtained at the MFA of the two-flavor NJL model will take the same value for $g_v^v = g_v^s$. In other words, the lattice curvature difference between the κ_i and κ_q can be regarded as an useful evidence for the unequal vector coupling strengths.

Since the two-flavor lattice calculation in [28] indicates that the κ_i is less than the κ_q , we thus infer that the g_v^v may be larger than the g_v^s near the chiral phase boundary for zero and small quark chemical potential. Following the spirit of Ref. [13], our numerical study suggests that the g_v^v is about 10% larger than the g_v^s near T_c according to the lattice curvatures in [28]. This conclusion is quite different from the estimation given in (7).

D. Constraints on the vector interactions from the couplings of vector mesons to nucleons and lattice susceptibilities

In Ref. [23], it is argued that the ratio of the couplings of ω and ρ mesons to nucleons can be used as a constraint on the vector coupling difference. In the chirally broken phase, the empirical value for this ratio is given by $g_{\omega NN}/g_{\rho NN} \simeq 3$, whereas in the chirally symmetric phase it is expected to be one. It is then proposed that the ratio g_v^v/g_v^s is located in the range from 1/3 to 1. The study in [23] also suggests that the flavor off-diagonal susceptibility for vanishing chemical potential is very sensitive to the vector coupling difference.

In addition, another quite similar estimation is given in Ref. [24], where the vector coupling difference is expressed as the function of two susceptibilities χ_q and χ_I under some assumptions. Using the lattice data for these susceptibilities as input, it is found that the g_v^v is always less than the g_v^s : their difference is quite large below T_c which approaches zero rapidly above T_c for zero chemical potential.

All the arguments given in the above subsections suggest that the vector interactions are repulsive (namely, g_v^s and g_v^v are all positive), but the relation between the g_v^s and g_v^v remains uncertain. Usually, the two vector couplings in the NJL model must take almost the same strength to reproduce the vacuum masses of the ω and ρ mesons at the MFA. However, the description of vector meson properties within the NJL formalism is not quite reliable since the momentum cutoff is not large enough compared to the ω and ρ masses. In addition, the T - μ dependence of the vector couplings is also unknown. Due to these uncertainties, the g_v^s and g_v^v in the Lagrangian

(4) will be treated as the free parameters in the following study.

III. VECTOR-INTERACTION INDUCED FLAVOR-MIXING AND THE THERMAL DYNAMICAL POTENTIAL AT FINITE BARYON AND ISOSPIN CHEMICAL POTENTIALS

In this section, we shall demonstrate that the vector coupling difference can lead to non-anomaly flavor-mixing at finite baryon and isospin densities.

The full Lagrangian of two-flavor NJL model with the interaction (4) reads

$$\mathcal{L} = \bar{\psi} (i\partial_\mu \gamma^\mu + \gamma_0 \hat{\mu} - \hat{m}_0) \psi + \mathcal{L}_{\text{eff}}^{(4)}, \quad (11)$$

where the quark chemical potentials are introduced and $\hat{m}_0 = \text{diag}(m_u, m_d)$ is the current quark matrix. We shall adopt the isospin symmetric quark masses with $m_u = m_d \equiv m_0$. The $\hat{\mu}$ in the Lagrangian (11) is the matrix of the quark chemical potentials which takes form

$$\hat{\mu} = \begin{pmatrix} \mu_u & \\ & \mu_d \end{pmatrix} = \begin{pmatrix} \mu - \mu_I & \\ & \mu + \mu_I \end{pmatrix}, \quad (12)$$

with

$$\mu = \frac{\mu_u + \mu_d}{2} = \frac{\mu_B}{3} \quad \text{and} \quad \mu_I = \frac{\mu_u - \mu_d}{2} = \frac{\delta\mu}{2}. \quad (13)$$

In (13), μ_B (μ_I) is the baryon (isospin) chemical potential, which corresponds to the conserved baryon (isospin) charge. In our notations, the μ_I refers to half of the difference between the μ_u and μ_d .

At finite densities, the quark chemical potentials are shifted by the vector interactions. Here we use μ' to denote the modified quark chemical potential. Note that the u quark density is different from the d quark one under the isospin asymmetry. Considering this point, the shifted quark chemical potentials take the form

$$\begin{aligned} \mu'_{u(d)} &= \mu_{u(d)} - 2g_v^s(\rho_u + \rho_d) - 2g_v^v(\rho_{u(d)} - \rho_{d(u)}) \\ &= \mu_{u(d)} - 2(g_v^s + g_v^v)\rho_{u(d)} - 2(g_v^s - g_v^v)\rho_{d(u)}, \end{aligned} \quad (14)$$

or

$$\mu' = \mu - 2g_v^s(\rho_u + \rho_d), \quad \mu'_I = \mu_I - 2g_v^v(\rho_u - \rho_d), \quad (15)$$

where

$$\rho_{u(d)} = \langle \psi_{u(d)}^\dagger \psi_{u(d)} \rangle \quad (16)$$

is the u (d) quark number density. Eq. (14) clearly shows that due to the vector coupling difference, not only the ρ_u but also the ρ_d give contribution to the effective chemical potential of u quark, and vice versa. This implies that the flavor-mixing arises at the MFA due to the vector interaction. As mentioned, this mixing has nothing to do with the axial anomaly. The modified chemical potentials

can also be rearranged as Eq. (15), which indicates that μ and μ_I are shifted by the isoscalar and isovector vector interactions, respectively.

Formally, the non-anomaly flavor-mixing shown in (14) for the modified chemical potentials is quite similar to the anomaly flavor-mixing for the constituent quark masses induced by the instantons, namely

$$M_{u(d)} = m_0 - 4g_{s1}\phi_{u(d)} - 4g_{s2}\phi_{d(u)}, \quad (17)$$

where

$$\phi_{u(d)} = \langle \bar{\psi}_{u(d)} \psi_{u(d)} \rangle \quad (18)$$

is the u (d) quark condensate. So at finite μ_I , the four-fermion interactions in (4) can give rise to two types of flavor-mixing at the MFA for non-vanishing δg_v and g_{s2} .

Using the conventional technique, the mean field thermal dynamical potential of the Lagrangian (11) at finite temperature and chemical potentials is expressed as

$$\begin{aligned} \Omega(T, \mu_u, \mu_d) = & \sum_{f=u,d} \Omega_0(T, \mu'_f; M_f) + 2g_{s1}(\phi_u^2 + \phi_d^2) + 4g_{s2}\phi_u\phi_d \\ & - (g_v^s + g_v^v)(\rho_u^2 + \rho_d^2) - 2(g_v^s - g_v^v)\rho_u\rho_d, \end{aligned} \quad (19)$$

where $\Omega_0(T, \mu'_f; M_f)$ is the contribution of a quasi-particle gas of the flavor f which takes the form

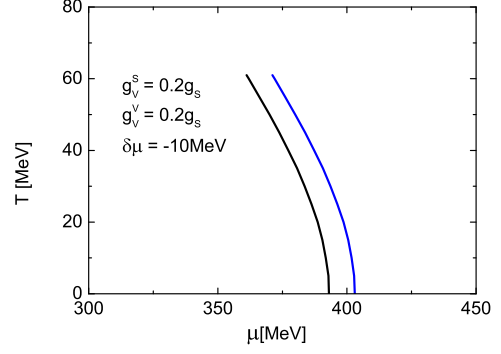
$$\begin{aligned} \Omega_0(T, \mu'_f; M_f) = & -2N_c T \int \frac{d^3p}{(2\pi)^3} \left[\ln[1 + \exp(-(E_f - \mu'_f)/T)] \right. \\ & \left. + \ln[1 + \exp(-(E_f + \mu'_f)/T)] \right] \\ & - 2N_c \int \frac{d^3p}{(2\pi)^3} E_f \theta(\Lambda^2 - \vec{p}^2), \end{aligned} \quad (20)$$

with the quasi-particle energy $E_f = \sqrt{\vec{p}^2 + M_f^2}$. The Λ in (20) is the parameter of three-momentum cutoff in the NJL model. We see that besides the modified chemical potential μ'_f , the flavor-mixing due to the vector coupling difference is also explicitly demonstrated in (19) via the direct coupling between the ρ_u and ρ_d . This is also analogous to the instanton induced flavor-mixing: in addition to the constituent mass M_f , the u quark condensate couples directly to the d quark one, which is also shown in (19).

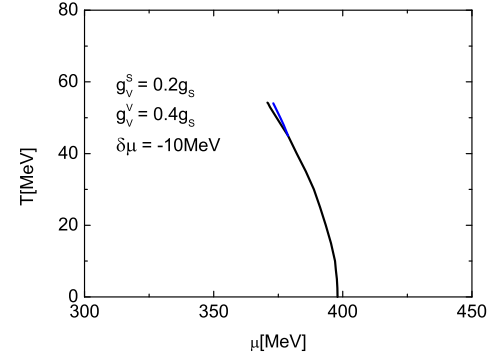
Minimizing the thermal dynamical potential (19), the motion equations for the mean fields ϕ_u , ϕ_d , ρ_u and ρ_d are determined through the coupled equations

$$\frac{\partial \Omega}{\partial \phi_u} = 0, \quad \frac{\partial \Omega}{\partial \phi_d} = 0, \quad \frac{\partial \Omega}{\partial \rho_u} = 0, \quad \frac{\partial \Omega}{\partial \rho_d} = 0. \quad (21)$$

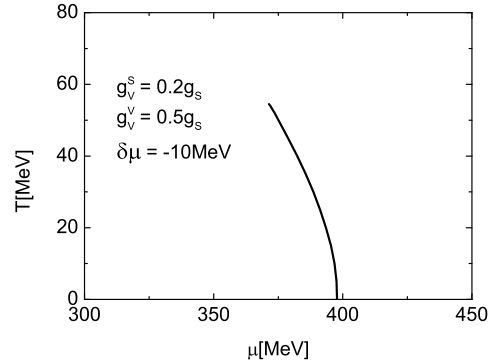
This set of equations is then solved for the fields ϕ_u , ϕ_d , ρ_u and ρ_d as functions of the temperature and chemical potentials. When there exist multi roots of these coupled equations, the solution corresponding to the minimal thermodynamical potential is favored.



(a)



(b)

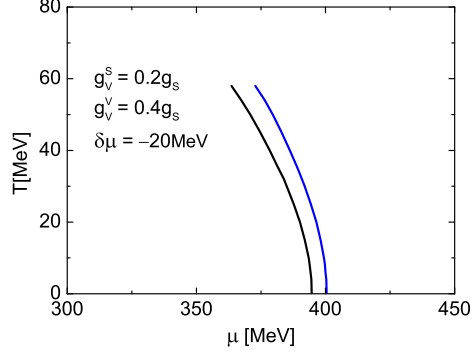


(c)

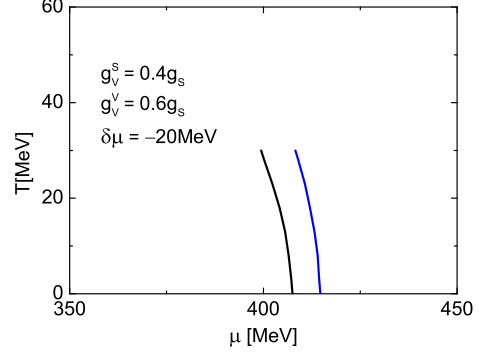
FIG. 1: The T - μ phase diagrams for varied vector-isovector coupling g_v^v at $\delta\mu = -10$ MeV without the axial anomaly. The vector-isoscalar coupling is fixed as $g_v^s = 0.2g_s$ (the g_s is the scalar coupling). The solid line stands for the first-order chiral boundary.

IV. CHIRAL PHASE TRANSITION UNDER THE INFLUENCE OF MISMATCHED VECTOR INTERACTIONS

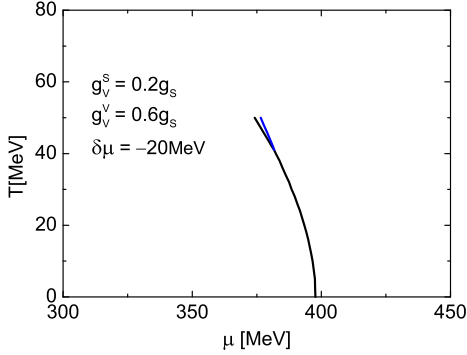
As mentioned, the separate chiral transitions because of finite μ_I [3, 4] can be removed by the flavor-mixing induced by the axial anomaly [14]. Since the instanton density may be suppressed significantly near the phase



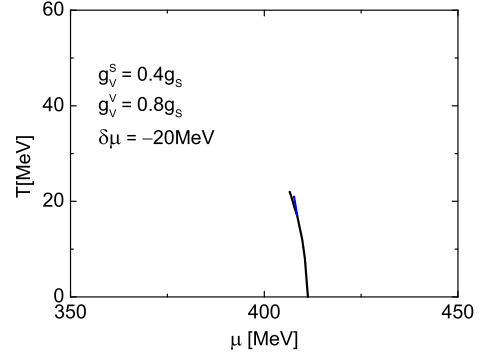
(a)



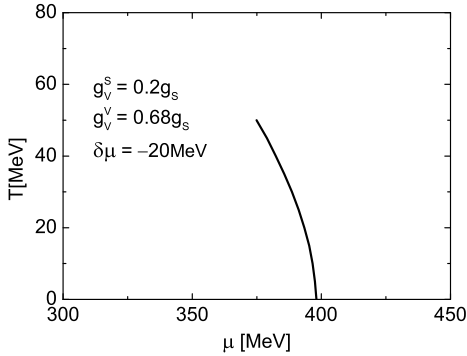
(a)



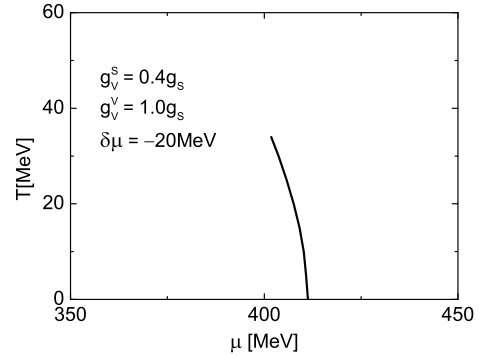
(b)



(b)



(c)



(c)

FIG. 2: The T - μ phase diagrams for varied vector-isovector coupling g_v^v at $\delta\mu = -20$ MeV without the axial anomaly. The fixed vector-isoscalar coupling g_v^s is the same as in Fig. 1. The solid line stands for the first-order chiral boundary.

boundary, we revisit this problem by taking into account the non-anomaly flavor-mixing due to the mismatched vector interactions. We shall check whether the emergence of the two critical endpoints is sensitive to the couplings g_v^s and g_v^v . In addition, the so called chiral equivalence at finite μ and μ_I is also checked in the MFA of NJL model by including the vector interactions.

For comparison, we follow the notations in Ref. [14] and introduce two parameters α and g_s which are defined

FIG. 3: The T - μ phase diagrams for varied vector-isovector coupling g_v^v at $\delta\mu = -20$ MeV without the axial anomaly. The vector-isoscalar coupling is fixed as $g_v^s = 0.4$ (relative to the scalar coupling g_s). The solid line stands for the first-order chiral boundary.

as

$$g_{s1} = (1 - \alpha)g_s, \quad g_{s2} = \alpha g_s. \quad (22)$$

Here the α means the ratio of the KMT interaction in the scalar-pseudoscalar channel, which is treated as a free parameter in the following calculations. The other model parameters, namely the current quark mass m_0 , the scalar coupling constant g_s and the three-momentum

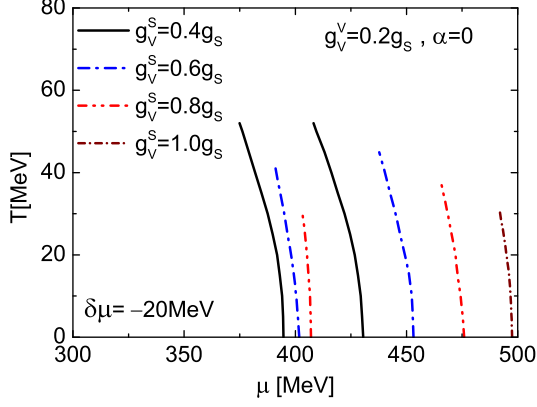


FIG. 4: The T - μ phase diagrams for varied vector-isoscalar coupling g_v^s at $\delta\mu = -20$ MeV. The vector-isovector coupling is fixed as $g_v^v = 0.2$ (relative to the scalar coupling g_s). The axial anomaly is ignored. All the lines stand for the first-order chiral boundaries.

cutoff Λ are all adopted from [14], which take the values

$$m_0 = 6 \text{ MeV}, \quad \Lambda = 0.590 \text{ GeV}, \quad g_s \Lambda^2 = 2.435. \quad (23)$$

These parameters are fixed by the pion mass, the pion decay constant, and the chiral condensate of the QCD vacuum.

A. Fate of separate chiral transitions under the weak isospin asymmetry without the axial anomaly

The role of the mismatched vector interactions on the separation of the chiral transition at finite T - μ under the weak isospin asymmetry is first investigated by switching off the KMT interaction. We focus on whether the two critical endpoints found previously could be ruled out by the non-anomaly flavor-mixing without the help of the axial anomaly.

We first study the cases for $g_v^v > g_v^s$ with a fixed small coupling $g_v^s = 0.2g_s$ under the rather weak isospin asymmetry $\delta\mu = -10$ MeV (Note that the μ_I defined in [14] corresponds to the $\delta\mu$ in our notations). The T - μ phase diagrams for varied g_v^v are shown in Fig. 1. For $g_v^v = g_v^s$, Fig. 1.(a) shows two separate first-order phase boundaries, which correspond to the chiral transitions for the u and d quarks, respectively. This is natural because of the decouple of the u and d quarks. For $g_v^v = 0.4g_s$, Fig. 1.(b) shows that only one first-order chiral boundary emerges at the low temperature, but it splits into two lines at the relatively higher temperature. So there are still two critical endpoints. Further increasing g_v^v to $0.5g_s$, Fig. 1.(c) displays that only one phase boundary appears. So we really observe that the two separate phase boundaries can

be changed into one by the non-anomaly flavor-mixing induced by the mismatched vector interactions.

We then increase the isospin asymmetry to $\delta\mu = -20$ MeV with the g_v^s unchanged (The typical value of $\delta\mu$ in heavy ion collisions may be within this range, as estimated in [14]). We obtain the similar phase diagrams by varying the g_v^v , which are displayed in Fig. 2. Compared to Fig. 1, a more large vector coupling difference is needed to convert the two phase boundaries into one because of the enhanced isospin asymmetry.

The above calculation for $\delta\mu = -20$ MeV is further extended to a fixed moderate coupling $g_v^s = 0.4g_s$. The phase diagrams for varied g_v^v with $g_v^v > g_v^s$ are shown in Fig. 3, which is still analogous to Fig. 1. In contrast to Fig. 2, a more strong g_v^v is required for the conversion of the two phase transitions into one due to the enlarged g_v^s . Fig. 3 also shows that the chiral transition is first softened and then strengthened with g_v^v . By comparison, the chiral transition is always weakened with the increase of g_v^s .

So for the weak isospin asymmetry, Figs. 1-3 show that the chiral transition separation can be removed by the mismatched vector interactions, even without the instanton induced flavor-mixing. Actually, all the three sets of phase diagrams in Figs. 1-3 are quite similar to Fig. 2 in Ref. [14] obtained by changing the α . In this sense, the non-anomaly flavor-mixing due to the vector coupling difference plays the similar role as the KMT interaction.

However, Figs. 1-3 indicate that the g_v^v must be much stronger than the g_v^s for turning the two chiral transitions into one: the g_v^v is at least twice as strong as the g_v^s to remove the separation. Of course, the fate of the separate chiral transitions depends on not only the vector coupling difference, but also the magnitudes of g_v^v and g_v^s . Here we do not show the results for $g_v^v > g_v^s$ with a fixed strong g_v^s since in this case only crossover transition appears.

On the contrary, we don't find the coincidence of the detached phase boundaries for $g_v^v < g_v^s$. In Fig. 4, we show the phase diagrams for $\delta\mu = -20$ MeV with varied g_v^s and fixed coupling $g_v^v = 0.2g_s$. We see that the two separate phase boundaries get farther rather than closer with the increase of $|\delta g_v|$ for $g_v^v < g_v^s$, which is quite different from what shown in Figs. 1-3.

The reason can be traced aback to Eqs. (14) and (15). First, according to Eq. (15), the $|\mu'_I|$ is explicitly less than the $|\mu_I|$ since the signs of μ_I and $-2g_v^v(\rho_u - \rho_d)$ in μ'_I are different for $g_v^v > 0$. So for $g_v^v > g_v^s$ with a fixed g_v^s , increasing g_v^v implies not only the enhancement of the flavor-mixing but also the reduction of $|\mu'_I|$ (see Fig. 7 in next subsection). This is why the two phase boundaries approach each other with the g_v^v , as shown in Figs. 1-3. Second, near the left side of the right phase boundary, the ρ_d is remarkably larger than the ρ_u because of the significant suppression of the d quark mass; but around the left side of the left phase boundary, the difference between the ρ_d and ρ_u is relatively small. So for $g_v^s > g_v^v$, the flavor-mixing term $-(g_v^s - g_v^v)\rho_d$ in μ'_u impacts the right phase boundary more significantly in contrast to

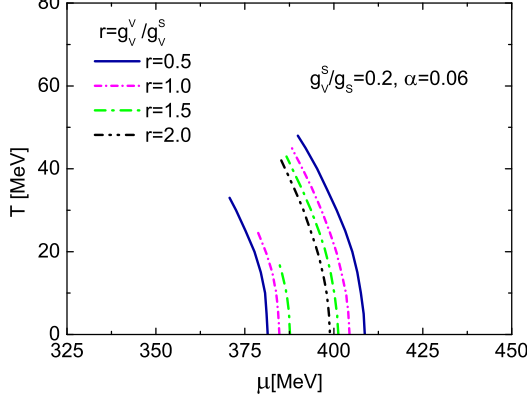


FIG. 5: The first order chiral boundaries in the T - μ plane for varied vector-isovector coupling g_v^v at $\delta\mu = -60$ MeV. The parameter α for the KMT interaction and vector-isoscalar coupling g_v^s are fixed as 0.06 (about one third of the vacuum value) and 0.2 (relative to the scalar coupling g_s), respectively.

what the corresponding term $-(g_v^s - g_v^v)\rho_u$ in μ_d' does on the left phase boundary, according to Eq. (14). This is why the right phase boundary moves more rapidly towards the higher μ with g_v^v in contrast to the left one, as shown in Fig. 4.

If g_v^s or/and g_v^v are strong enough, the first-order chiral transition will change into crossover and it would be no critical point. Owing to the vector interactions, it is possible that one of the two phase boundaries first disappears while the other one still remains with the change of the vector interactions (In contrast, the two critical endpoints always appear at the same temperature in Ref. [3, 4]). Such a case is really observed in Fig. 4 for very strong vector interaction $g_v^s = 1.0g_s$. In the next subsection, we will show that the emergence of only one critical endpoint via this manner does not require very strong vector interaction when the weak KMT interaction is included.

B. Fate of separate chiral transitions at finite μ_I under the influence of both vector interactions and the axial anomaly

In Ref. [14], it is found that the separate chiral transitions at fixed $\delta\mu=60$ MeV³ only appear for $\alpha < \alpha_c = 0.12$, where the critical value α_c is argued to be less than the vacuum α . Here, we assume that the physical α near

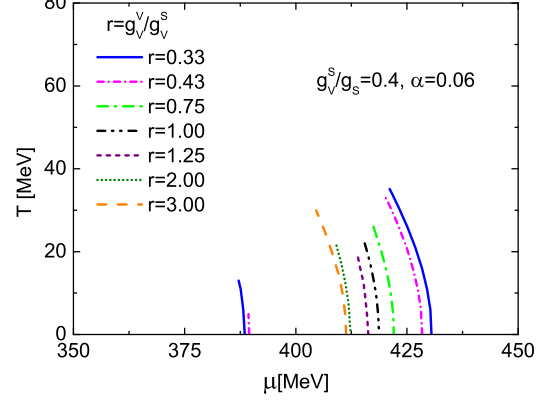


FIG. 6: The first order chiral boundaries in the T - μ plane for varied vector-isovector coupling g_v^v at $\delta\mu = -60$ MeV. The parameter α for the KMT interaction and vector-isoscalar coupling g_v^s are fixed as 0.06 (about one third of the vacuum value) and 0.4 (relative to the scalar coupling g_s), respectively.

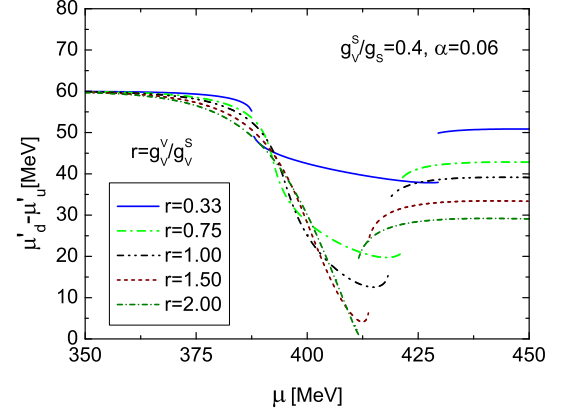


FIG. 7: The difference between the effective chemical potentials of u and d quarks as a function of μ for varied vector-isovector coupling g_v^v at $\delta\mu = -60$ MeV and $T = 10$ MeV. The vector-isoscalar coupling g_v^s and parameter α for the KMT interaction are fixed as 0.4 (relative to the scalar coupling g_s) and 0.06 (about one third of the vacuum value), respectively.

the phase boundary is obviously less than the α_c due to the effective suppression of instantons. We shall concentrate on whether the two critical endpoints could still appear under the same isospin asymmetry as in Ref. [14] by including the vector interactions. For comparison, the $\delta\mu$ is fixed as -60 MeV in our numerical study (Changing

³ The chiral transition with the same $\delta\mu$ is also studied in [4] in a NJL type model, where the axial anomaly is ignored.

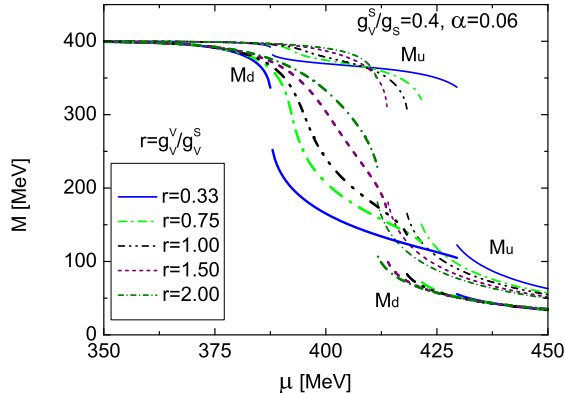


FIG. 8: The u and d quark masses as functions of μ for varied vector-isovector coupling g_v^v at $\delta\mu = -60$ MeV and $T = 10$ MeV. The vector-isoscalar coupling g_v^s and parameter α for the KMT interaction are the same as in Fig. 7.

the sign of $\delta\mu$ does not alter the conclusion since it only indicates the interchange of u and d quarks.). We choose a comparatively weak KMT interaction with $\alpha = 0.06$, which is half of the α_c or about one third of the vacuum α given in [14].

We still first study the chiral phase transition for a fixed weak coupling $g_v^s = 0.2g_s$ by varying the g_v^v . The corresponding phase diagrams are shown in Fig. 5. We see that the separate first-order chiral transitions still appear for the small coupling $g_v^v = 0.1g_s$. With raising g_v^v , the two phase boundaries get closer and shorter. We notice that the left phase boundary shortens more significantly with g_v^v compared to the right one. For the moderate coupling $g_v^v = 0.4g_s$, the left phase boundary eventually vanishes (totally turns into crossover) but the right one still survives. So due to the vector interactions, the separation of the chiral transition can still be removed even the α is obviously less than the α_c .

The investigation is then extended to a fixed moderate coupling $g_v^s = 0.4g_s$, with both $\delta\mu$ and α unchanged. We obtain the qualitatively similar phase diagrams for varied g_v^v as displayed in Fig. 6. We see that a rather weak coupling $g_v^v = 0.45g_s^s$ is already strong enough to change the left phase boundary into crossover due to the raised g_v^s . It indicates that the g_v^v does not need to be larger than the g_v^s for the emergence of only one critical endpoint. Fig. 6 also shows that the right phase boundary first shortens and then elongates with g_v^v , but the left one always gets shorter with g_v^v until it vanishes. Our further numerical calculations suggest that the single phase boundary can even survive for very strong $g_v^v = 1.5g_s$.

Similar to Figs. 1-3, Figs. 5-6 display that the two separate phase boundaries approach each other with the increase of g_v^v . As mentioned, this is due to the decrease of

$|\delta\mu'|$ with g_v^v . To illustrate this point, the μ -dependence of $|\delta\mu'|$ for varied g_v^v at $T = 10$ MeV are shown in Fig. 7, where the g_v^s and $\delta\mu$ are the same as that in Fig. 6. We see that compared to the $|\delta\mu|$, the $|\delta\mu'|$ in between the left critical (or pseudo-critical) chemical potential and the right one reduces dramatically with g_v^v .

Distinct from Figs. 1-3 (and Fig. 2 in [14]), Figs. 5-6 exhibit that with increasing g_v^v it is the transition of one phase boundary into crossover rather than the coincidence of the two which results in only one critical endpoint. This is because the left chiral transition for d quark is softened more significantly by both g_v^v and α . First, raising g_v^v leads to the decrease (increase) of the $\mu'_{d(u)}$ according to Eq. (14). So the left chiral transition for d quark is weakened more significantly with g_v^v compared to the right one for u quark. This point is also clearly demonstrated in Fig. 8, where the quark masses as functions of μ at $T = 10$ MeV are plotted. Note that even μ'_u raises with g_v^v for a fixed g_v^s , it does not mean that the right chiral transition for u quark must be intensified. Actually, Figs. 5-6 show that the right chiral transition is softened slightly with g_v^v up to a moderate coupling strength (The reason will be given below). Second, around the left phase boundary, the u quark condensate is still sizable and thus makes a relatively large contribution to the d quark mass via the anomaly-related flavor-mixing. In contrast, near the right phase boundary, the d quark condensate is suppressed significantly and thus its contribution to the u quark mass is relatively small. This implies that the left chiral transition for d quark is also weakened more notably by the KMT interaction⁴. This is why the left chiral boundary disappears (totally turns into crossover) but the right one still remains for weak α and moderate (or weak) g_v^v .

Compared to the case with $\alpha = 0$, Figs. 5-6 demonstrate that it is not the vector coupling difference but the strength of g_v^v which is crucial for the appearance of a single critical endpoint. Especially, even only one phase boundary appears in Figs. 5-6 for weak and moderate g_v^v , the d quark mass has reduced significantly near the left side of the true phase transition, as displayed in Fig. 8. This is different from what shown in Fig. 2 of [14] for $\alpha > \alpha_c$, where both masses of u and d quarks drop suddenly from large values to small ones across the phase boundary.

Let us explain why the right chiral transition for u quark is also weakened slightly with g_v^v up to a moderate strength. The reason can be attributed to the abrupt increase of ρ_u and the relatively mild change of ρ_d near the right phase boundary. To understand this point, we can make a rough estimate of the variation of μ'_u at the right

⁴ Here the contribution of u quark condensate to the d quark mass can be regarded as an effective increase of the current mass of d quark, and vice versa. So the chiral phase transition for d quark is softened by the KMT interaction.

critical chemical potential μ_c at $T = 0$ (we use $\rho_f^{l(r)}$ and $\mu_f^{l(r)}$ to denote the quark density and chemical potential on the left (right) side of μ_c , respectively). The effective u quark chemical potential on the left side of μ_c can be approximated as $\mu_u^l \approx \mu_c + \mu_I - 2g_v^s \rho_d^l + 2g_v^v \rho_d^l$ according to Eq. (15) since $\rho_d^l \gg \rho_u^l \approx 0$. Similarly, on the right side of μ_c , we obtain $\mu_u^r \approx \mu_c + \mu_I - 2g_v^s \rho_d^r - 2g_v^v \rho_d^r$ using the approximations $\rho_u^r \approx \rho_d^r \approx \rho_d^l$. These simplified expressions indicate that the μ_u^l raises with g_v^v while the μ_u^r remains the same. In general, on the same side of μ_c , the larger the μ_u^l , the smaller the u quark mass. So that the μ_u^l increases evidently but the μ_u^r keeps almost unchanged with g_v^v imply that the abrupt drop of u quark mass at μ_c is weakened.

Note that such an explanation only holds for weak and moderate g_v^v , as exhibited in Fig. 8. This is because the approximations $\rho_d^r \approx \rho_d^l$ and $\rho_d^l \gg \rho_u^l$ adopted above are no longer proper for the strong g_v^v since near the μ_c the m_d^l becomes significantly larger than the m_d^r and the gap between the m_u^l and m_d^l also reduces obviously due to the decrease of $|\mu_u^l|$. Actually, Fig. 8 shows that for the strong coupling $g_v^v = 0.8g_s$ the abrupt change of u quark mass across the phase boundary is not weakened but strengthened compared to the case for $g_v^v = 0.6g_s$, which is consistent with the decrease of μ_u^l with g_v^v .

We stress that Fig. 8 also shows that the crossover chiral transition for d quark becomes less and less obvious with g_v^v , especially for $g_v^v > g_v^s$. The reason is that besides the influence of the α and the increased g_v^v , the crossover is also softened by the flavor-mixing due to the vector coupling difference. We see that the chiral transition for the strong coupling $g_v^v = 0.8g_s$ is already the type displayed in Fig. 2 of [14] for $\alpha > \alpha_c$: Namely, the only phase boundary can still be regarded as the coincidence of the left and right first-order transition lines driven by the vector and KMT interactions. Unlike the case for zero α , the flavor-mixing due to the vector coupling difference plays a relatively minor role here even the chosen α is just about one third of its vacuum value. Or in other words, the flavor-mixing due to vector interactions is unnecessary for the only phase boundary if the g_v^v is strong enough and the KMT interaction is not very weak.

In Ref. [13], it is argued that the ratio g_v^s/g_s in a Polyakov-loop extended three-flavor NJL model is likely to be larger than 0.4. As mentioned, our numerical study suggests that the g_v^v obtained using the same method is about 10% larger than the g_v^s according to the recent two-flavor lattice data. If such an estimation is reliable, our model study suggests that the separate chiral transitions due to the isospin asymmetry may be still impossible in heavy ion collisions if the axial anomaly is suppressed effectively but not very significantly near the phase boundary. Actually, Fig. 6 shows that even the weak coupling strength $g_v^v = 0.2g_s$ is already strong enough to change the left phase boundary for d quark to a rapid crossover

for the moderate coupling $g_v^s = 0.4g_s$ ⁵. In addition, even it is proposed in [23] that ratio g_v^v/g_v^s may locate in the range 1/3 and 1, it is argued in [24] that this value rapidly approaches to 1 for $T > T_c$. All these arguments support that the g_v^v may not be very weak near the phase boundary, at least for small density. So even our choice of the α is just half of the α_c or one third of its vacuum value, the main conclusion for $\alpha > \alpha_c$ in [14] may still hold owing to the vector interactions.

All the above calculations are performed by changing the g_v^v or g_v^s with the α unchanged. Instead, we can do the same calculations by fixing the g_v^v and g_v^s and varying the α . We then observe that the critical value of the α for the disappearance of the separation of the chiral transition reduces significantly compared to the α_c obtained in Ref. [14] if the vector interactions are not very weak (especially the g_v^v). Of course, if both g_v^s and g_v^v are all strong, there is only the crossover transition no matter to what degree the axial anomaly is suppressed.

C. Validity of phase quenching in mean field NJL model with mismatched vector interactions

Recently, the equivalence of QCD at finite μ and μ_I with a large number of colors N_c has been proposed [18, 19, 31]. The equivalence may enable the people to study the properties of QCD at finite μ via the calculations of lattice QCD at finite μ_I . The detailed discussion on the validity of the phase quenching outside of the pion condensation region has been given in Ref. [19], where the equivalence is confirmed in several popular QCD models at the MFA. Especially, it is argued that the phase quenching still holds at the MFA of the NJL model even taking into account the flavor-mixing induced by instantons.

One evidence for the validity of phase quenching in [19] is that the free energies at finite μ and μ_I are identical at the MFA in these QCD models, namely

$$\Omega_M(\mu_u = \mu_0, \mu_d = \mu_0, T) = \Omega_M(\mu_u = \mu_0, \mu_d = -\mu_0, T), \quad (24)$$

where μ_0 and T are located in the region without pion condensation. In Ref. [19], such an equality is also obtained in the NJL model without considering the vector interactions. Here we stress that the relation (24) is still valid if vector interactions with the same couplings are included. This is because even the quark chemical potentials for u and d are modified, they are shifted by quantities with the same magnitude due to the relations $\rho_B|_{\mu_I=0} = \rho_I|_{\mu=0}$ and $\rho_u|_{\mu_I=0} = -\rho_d|_{\mu=0}$ for $g_v^v = g_v^s$. So if the one-gluon exchange type interaction used in [19] is

⁵ This value locates in the range of $0.25g_s$ and $0.5g_s$, which are obtained from the instanton liquid molecule model [30] and the Fierz transformation of the one gluon exchange interaction, respectively

adopted by taking into account the vector channels, the phase quenching is still satisfied at the mean field level in the Hartree approximation. This is also consistent with the large- N_c analysis given in [19].

However, when considering the mismatched vector interactions, the phase quenching or the equivalence aforementioned becomes invalid in this model even at the MFA. The reason is that for finite μ and zero μ_I and finite μ_I and zero μ , the effective baryon and isospin chemical potentials are modified by the couplings g_v^s and g_v^v , respectively (see Eq. (15)). Consequently, the effective chemical potential $\mu'_u|_{\mu_I=0}$ is no longer equal to $-\mu'_d|_{\mu=0}$ and so the equality (24) does not hold again according to Eq. (19).

In this case, the degree of the equivalence breaking depends on the vector coupling difference. For instance, if $g_v^v = g_v^s/3$ as proposed in [23], the equivalence in the MFA will be violated seriously. In addition, the one-gluon exchange type interaction in the Hartree-Fock approximation indicates that the vector coupling difference is subleading in $1/N_c$ according to Eq. (6). So for $N_c = 3$, the phase quenching is also broken obviously for such an interaction in the MFA⁶. On the other hand, the constraints from the chiral curvatures in the lattice QCD calculations suggests that vector coupling difference is not so large near T_c at zero μ or μ_I . Such an estimation suggests that the deviation of the equivalence at the MFA will be not so significant in the NJL model, at least for small chemical potentials.

It is also interesting to investigate the violation of the phase quenching at the MAF in other QCD models. In particular, the similar study can be extended directly to the quark meson model [32] of QCD by including the vector interactions [33]. If the quark-vector couplings g_ω and g_ρ in [33] are different, the so called phase quenching at the MAF will be broken too in this model.

V. DISCUSSION AND CONCLUSION

We have studied the influence of vector interactions with different coupling constants in the isoscalar and isovector channels on the possible separation of the chiral transition under the isospin asymmetry in a two-flavor NJL model, where the $U(1)_A$ symmetry is assumed to be restored effectively near the phase boundary. In addition, the effect of the mismatched vector interactions on the proposed equivalence for the chiral transitions at finite μ and μ_I has also been studied at the MFA in this model.

We first show that, besides the argument based on the empirically different nucleon and vector-meson couplings [23], the one-gluon exchange type interaction can

also give rise to unequal vector interactions with $g_v^s > g_v^v$ at the MFA when including the Fock contribution. By extending the work [15] to finite μ_I , we then obtain the quite different vector coupling difference with $g_v^s < g_v^v$ from the constraints of lattice chiral curvatures at zero/small quark chemical potentials. We demonstrate that, similar to the mass-mixing induced by the KMT interaction, the density-mixing due to the modified quark chemical potentials is produced owing to the mismatched vector interactions.

For the weak isospin asymmetry, we find that to convert the two separate chiral transitions into one, the g_v^v must be significantly stronger than the g_v^s without the axial anomaly. In this case, the non-anomaly flavor-mixing induced by the vector interactions impacts the phase transition separation in the similar way as the anomaly one induced by instantons: the two detached phase boundaries get closer first and then coincide with the enhancement of the flavor-mixing. For the weak KMT interaction (the chosen coupling strength is about one third of the vacuum value) and relatively strong isospin asymmetry (the same as in [14]), we find that it is the strength of g_v^v rather than the vector coupling difference which is crucial for the only single phase boundary. In particular, the separate chiral transitions disappear for the moderate or even weak g_v^v , not because of the overlap of the two phase boundaries, but because of the conversion of the left one into crossover. This is distinct from what found in [14] for $\alpha > \alpha_c$ without the vector interactions and the aforementioned coincidence of the phase boundaries without the KMT interaction. The reason is that under the isospin asymmetry, the left chiral transition for d quark is softened more significantly by both the vector-isovector and KMT interactions and eventually turns into crossover in advance.

Physically, the g_v^v may not be much stronger than the g_v^s near the phase boundary. So even the mismatched vector interactions can lead to a non-anomaly flavor-mixing, its effect on the separation of the chiral transition is limited unless the $|\mu_I|$ is very small. This seems to indicate that the two critical endpoints due to finite μ_I are still possible and may be observed in heavy ion collisions if the KMT interaction is very weak. However, we remark that the effective restoration of the $U(1)_A$ symmetry obtained in recent lattice simulations does not imply that the effect of axial anomaly can be ignored near T_c . Actually, the remnant $U(1)_A$ breaking around T_c for zero density is still observed in these studies. On the other hand, the constraints from the lattice chiral curvatures and flavor susceptibilities all indicate that the strengths of g_v^v and g_v^s are considerable around T_c for zero density compared to the scalar interaction. We can expect that near the phase boundary at finite density, the KMT interaction may also not be very weak and the vector interactions are still appreciable. In this sense, the separate chiral transitions due to the isospin asymmetry could be still impossible in heavy ion collisions because of the vector interactions even the instanton effect may be suppressed

⁶ Note that the KMT interaction is also $1/N_c$ suppressed. However, the phase quenching is still exact at the MFA when the KMT interaction is included, as argued in [19].

effectively.

We also revisit the validity of the phase quenching in the MFA of the NJL model by including the vector interaction. We first confirm that the equivalence for the chiral transition at finite μ and μ_I out of the pion condensation region proposed by Hanada et al. is still valid at the MFA for $g_v^v = g_v^s$. We then point out that such an equivalence is broken explicitly by the mismatched vector interactions even at the MFA and the degree of this violation is dependent on the vector coupling difference.

Note that recently the Polyakov-Loop extended NJL model has been extensively used to investigate the thermal and dense properties of QCD. We stress that even our study is based on the NJL model, introducing the Polyakov-Loop dynamics does not qualitatively change our main conclusions. In addition, our study can be directly extended to the quark meson model of QCD by

incorporating the quark-vector-meson couplings and the axial anomaly.

In this paper, we only study the chiral transition at relatively small $|\mu_I|$. In the neutron star core, the isospin asymmetry required by the charge neutrality and β -equilibrium may not be so weak. Especially, for $|\mu_I| > m_\pi/2$, the pion condensed matter may appear [34–36]. Moreover, the color superconductivity is also not considered in our calculation. The roles of the mismatched vector interactions in these research topics deserve further investigations.

Acknowledgements

Z.Z. was partially supported by the NSFC (No.11275069), by the Fundamental Research Funds for the Central Universities of China, and by the University Plan of NCEPU for the Promotion of Arts and Sciences.

-
- [1] B. Mohanty [STAR Collaboration], J. Phys. G **38**, 124023 (2011) [arXiv:1106.5902 [nucl-ex]]; J. T. Mitchell [PHENIX Collaboration], Nucl. Phys. A **904-905**, 903c (2013) [arXiv:1211.6139 [nucl-ex]]; B. Mohanty, PoS CPOD **2013**, 001 (2013) [arXiv:1308.3328 [nucl-ex]].
 - [2] O. Philipsen, Prog. Part. Nucl. Phys. **70**, 55 (2013) [arXiv:1207.5999 [hep-lat]].
 - [3] B. Klein, D. Toublan and J. J. M. Verbaarschot, Phys. Rev. D **68**, 014009 (2003) [hep-ph/0301143].
 - [4] D. Toublan and J. B. Kogut, Phys. Lett. B **564**, 212 (2003) [hep-ph/0301183].
 - [5] M. Kitazawa, T. Koide, T. Kunihiro and Y. Nemoto, Prog. Theor. Phys. **108**, 929 (2002) [hep-ph/0207255, hep-ph/0307278].
 - [6] T. Hatsuda, M. Tachibana, N. Yamamoto and G. Baym, Phys. Rev. Lett. **97**, 122001 (2006) [arXiv:hep-ph/0605018].
 - [7] Z. Zhang, K. Fukushima and T. Kunihiro, Phys. Rev. D **79**, 014004 (2009) [arXiv:0808.3371 [hep-ph]].
 - [8] Z. Zhang and T. Kunihiro, Phys. Rev. D **80**, 014015 (2009) [arXiv:0904.1062 [hep-ph]]; Phys. Rev. D **83**, 114003 (2011) [arXiv:1102.3263 [hep-ph]].
 - [9] T. Kunihiro, Y. Minami and Z. Zhang, Prog. Theor. Phys. Suppl. **186**, 447 (2010) [arXiv:1009.4534 [nucl-th]].
 - [10] R. D. Pisarski and F. Wilczek, Phys. Rev. D **29**, 338 (1984).
 - [11] G. 't Hooft, Phys. Rev. D **14**, 3432 (1976) [Erratum-ibid. D **18**, 2199 (1978)]; G. 't Hooft, Phys. Rept. **142**, 357 (1986).
 - [12] M. Kobayashi and T. Maskawa, Prog. Theor. Phys. **44**, 1422 (1970).
 - [13] N. M. Bratovic, T. Hatsuda and W. Weise, Phys. Lett. B **719**, 131 (2013) [arXiv:1204.3788 [hep-ph]] and references therein.
 - [14] M. Frank, M. Buballa and M. Oertel, Phys. Lett. B **562**, 221 (2003) [hep-ph/0303109].
 - [15] A. Bazavov *et al.* [HotQCD Collaboration], Phys. Rev. D **86**, 094503 (2012) [arXiv:1205.3535 [hep-lat]].
 - [16] G. Cossu, S. Aoki, H. Fukaya, S. Hashimoto, T. Kaneko, H. Matsufuru and J. -I. Noaki, arXiv:1304.6145 [hep-lat].
 - [17] S. Aoki, H. Fukaya and Y. Taniguchi, Phys. Rev. D **86**, 114512 (2012) [arXiv:1209.2061 [hep-lat]].
 - [18] M. Hanada and N. Yamamoto, JHEP **1202**, 138 (2012) [arXiv:1103.5480 [hep-ph]].
 - [19] M. Hanada, Y. Matsuo and N. Yamamoto, Phys. Rev. D **86**, 074510 (2012) [arXiv:1205.1030 [hep-lat]].
 - [20] M. Asakawa, K. Yazaki, Nucl. Phys. A **504** (1989) 668.
 - [21] K. Fukushima, Phys. Rev. D **78**, 114019 (2008) [arXiv:0809.3080 [hep-ph]].
 - [22] T. Kunihiro, Phys. Lett. B **271**, 395 (1991).
 - [23] C. Sasaki, B. Friman and K. Redlich, Phys. Rev. D **75**, 054026 (2007) [hep-ph/0611143].
 - [24] L. Ferroni and V. Koch, Phys. Rev. C **83**, 045205 (2011) [arXiv:1003.4428 [nucl-th]].
 - [25] M. Takizawa, T. Kunihiro and K. Kubodera, Phys. Lett. B **237**, 242 (1990).
 - [26] K.P. Klevansky, Rev. Mod. Phys. **64**, 649 (1992).
 - [27] Z. Zhang, Phys. Rev. D **85**, 114028 (2012) [arXiv:1201.0422 [hep-ph]].
 - [28] P. Cea, L. Cosmai, M. D'Elia, A. Papa and F. Sanfilippo, Phys. Rev. D **85**, 094512 (2012) [arXiv:1202.5700 [hep-lat]].
 - [29] M. D'Elia and F. Sanfilippo, Phys. Rev. D **80**, 014502 (2009) [arXiv:0904.1400 [hep-lat]].
 - [30] T. Schafer and E. V. Shuryak, Rev. Mod. Phys. **70**, 323 (1998) [hep-ph/9610451].
 - [31] Y. Hidaka and N. Yamamoto, Phys. Rev. Lett. **108**, 121601 (2012) [arXiv:1110.3044 [hep-ph]].
 - [32] D. U. Jungnickel and C. Wetterich, Phys. Rev. D **53**, 5142 (1996) [hep-ph/9505267].
 - [33] H. Ueda, T. Z. Nakano, A. Ohnishi, M. Ruggieri and K. Sumiyoshi, Phys. Rev. D **88**, 074006 (2013) [arXiv:1304.4331 [nucl-th]].
 - [34] D. T. Son and M. A. Stephanov, Phys. Rev. Lett. **86**, 592 (2001); Phys. At. Nucl. **64**, 834 (2001).
 - [35] J. B. Kogut and D. K. Sinclair, Phys. Rev. D **66**, 034505 (2002); Phys. Rev. D **70**, 094501 (2004).
 - [36] L. -y. He, M. Jin and P. -f. Zhuang, Phys. Rev. D **71**, 116001 (2005) [hep-ph/0503272]; Z. Zhang and Y. -X. Liu, Phys. Rev. C **75**, 064910 (2007) [hep-ph/0610221]; Phys. Rev. C **75**, 035201 (2007) [hep-ph/0603252].